Loss of *Runx1* perturbs adult hematopoiesis and is associated with a myeloproliferative phenotype

Joseph D. Growney, Hirokazu Shigematsu, Zhe Li, Benjamin H. Lee, Jennifer Adelsperger, Rebecca Rowan, David P. Curley, Jeffery L. Kutok, Koichi Akashi, Ifor R. Williams, Nancy A. Speck, and D. Gary Gilliland

Homozygous loss of function of *Runx1* (Runt-related transcription factor 1 gene) during murine development results in an embryonic lethal phenotype characterized by a complete lack of definitive hematopoiesis. In light of recent reports of disparate requirements for hematopoietic transcription factors during development as opposed to adult hematopoiesis, we used a conditional gene-targeting strategy to effect the loss of *Runx1* function in adult mice. In contrast with the critical role of *Runx1* during development, *Runx1* was not essential for hematopoiesis in the adult hematopoietic compartment, though a number of significant hematopoietic abnormalities were observed. *Runx1* excision had lineage-specific effects on B- and T-cell maturation and pronounced inhibition of common lymphocyte progenitor production. *Runx1* excision also resulted in inefficient platelet production. Of note, *Runx1*-deficient mice developed a mild myeloproliferative phenotype characterized by an increase in peripheral blood neutrophils, an increase in myeloid progenitor populations, and extramedullary hematopoiesis composed of maturing myeloid and erythroid elements. These findings indicate that *Runx1* deficiency has markedly different consequences during development compared with adult hematopoiesis, and they provide insight into the phenotypic manifestations of *Runx1* deficiency in hematopoietic malignancies. (Blood. 2005;106: 494-504)

Introduction

RUNX1 (also known as *AML1*, *CBFA2,* and *PEPB2A*) encodes a heterodimeric partner of *CBFβ* (core-binding factor beta gene), and together they constitute a transcription factor in the core-binding factor (CBF) family. Runx1-CBFβ is required for hematopoietic stem cell emergence,[1,2] and it regulates a broad spectrum of genes in the myeloid and lymphoid lineages, including *IL3* (interleukin 3 gene), *CSF2* (colony-stimulating factor 2 [granulocyte-macrophage] gene), *CSF1R* (colony-stimulating factor 1 receptor gene), *CD4* (CD4 antigen gene), and *Tcrd* (T-cell receptor delta chain gene).[3-10] Mice that are deficient in either *Runx1* or *Cbfb* lack definitive hematopoiesis and die during midgestation, emphasizing the important role that CBF plays in development.[11-14] Recent expression studies using internal ribosomal entry site–green fluorescence protein (IRES-GFP) or *lacZ* knock-in mice further demonstrate the wide expression pattern of *Runx1* throughout the mature hematopoietic system and suggest lineage-specific requirements for *Runx1* expression in adult hematopoietic development.[15,16]

Several lines of evidence suggest that loss-of-function mutations in *RUNX1* contribute to the pathogenesis of myelodysplastic syndrome (MDS) and acute myeloid leukemia (AML). First, RUNX1 and its heterodimeric partner, CBFβ, are among the most common targets of chromosomal translocations in human leukemia. Three examples—t(8;21)(q22;q22),[17-21] inv[16](p13q22),[22] and t(12;21)(p13;q22),[23-25] giving rise to the *RUNX1-ETO* (eight to twenty-one), *CBFB-MYH11,* and *ETV6-RUNX1* fusion proteins, respectively—account for approximately 25% of adult AML and 25% of pediatric acute lymphoblastic leukemia (ALL).[26-34] Second, familial platelet disorder with propensity to develop acute myeloid leukemia (FPD/AML; MIM 301699) is an autosomal dominant disorder that is caused by loss-of-function mutations in *RUNX1*[35,36] and that has phenotypic similarities to MDS, including peripheral blood cytopenias, decreased colony-forming activity in myeloid progenitors, qualitative and quantitative platelet defects, and high likelihood of progression to AML during the lifetime of affected persons. Third, mutations in *RUNX1* have been identified in sporadic leukemias at a frequency of approximately 3% to 5% and at a lower frequency in MDS. Mutations in *RUNX1* are more common in undifferentiated myeloid leukemias (French-American-British [FAB] subtype M0), occurring at a frequency of approximately 25%, and in AML associated with trisomy 21.[37] Most sporadic cases of AML with loss-of-function mutations in *RUNX1* have biallelic mutations.[38]

Translocations that target CBF result in the expression of fusion proteins lacking the ability to transactivate expression of hematopoietic target genes.[39-42] Furthermore, homologous recombination in which the *RUNX1/ETO* and *CBFB/MYH11* alleles

From the Division of Hematology and the Department of Pathology, Brigham and Women's Hospital, Boston; Cancer Immunology and AIDS, Dana-Farber Cancer Institute, Boston; Howard Hughes Medical Institute, Harvard Medical School, Boston, MA; Department of Biochemistry, Dartmouth Medical School, Hanover, NH; and Department of Pathology, Emory University, Atlanta, GA.

Submitted August 26, 2004; accepted March 16, 2005. Prepublished online as *Blood* First Edition Paper, March 22, 2005; DOI 10.1182/blood-2004-08-3280.

Supported in part by the American Cancer Society (postdoctoral fellowship grant PF-02-133-01-LIB) (J.D.G.), the Public Health Service (grant R01CA58343) (N.A.S.), the National Cancer Institute (grant CA66996), the National Institute of Diabetes and Digestive and Kidney Diseases (grant 50564), and the Leukemia and Lymphoma Society (D.G.G.). The transgenic mouse facility at Dartmouth is supported in part by a core grant from the Norris Cotton Cancer Center. D.G.G is an Investigator for the Howard Hughes Medical Institute.

Reprints: D. Gary Gilliland or Joseph D. Growney, Division of Hematology, Brigham and Women's Hospital, 1 Blackfan Circle, Boston, MA 02115; e-mail: ggilliland@rics.bwh.harvard.edu or jgrowney@rics.bwh.harvard.edu.

The publication costs of this article were defrayed in part by page charge payment. Therefore, and solely to indicate this fact, this article is hereby marked "advertisement" in accordance with 18 U.S.C. section 1734.

were "knocked-in" to the *Runx1* or *Cbfb* loci, respectively, resulted in midgestation embryonic lethality with a phenotype that was nearly identical to that of mice with homozygous deficiency of either *Runx1* or *Cbfb,* demonstrating that *RUNX1/ETO* and *CBFB/MYH11* are dominant-negative *Runx1* and *Cbfb* alleles.[43-45] Collectively, these data indicate that loss of function of CBF, either because of chromosomal translocations or because of loss-of-function point mutations, contributes to the pathogenesis of AML in part by interfering with normal hematopoietic differentiation programs.

Thus, there is a paradox that *RUNX1* function is required for definitive hematopoiesis, yet *RUNX1* loss of function is associated with acute leukemias in which hematopoietic progenitors have self-renewal capacity. There are now a number of examples of disparate requirements for hematopoietic transcription factors during development compared with adult hematopoiesis. For example, *Scl* (*Tal1*) (the T-cell lymphocyte leukemia 1 gene) is essential for hematopoietic development during embryogenesis but is dispensable for adult hematopoiesis.[46-48] To further characterize the role of *Runx1* in adult hematopoiesis and in leukemia, we generated a conditional *Runx1* allele that would allow for analysis of the role of *Runx1* in the adult hematopoietic compartment.

Materials and methods

Generation of the conditional *Runx1* mouse strain

A 4.3-kilobase (kb) *Xba*I-*Avr*II genomic fragment upstream of exon 4 of *Runx1* and a 3.0-kb *Afl*II-*Xho*I fragment downstream of exon 4 were introduced as the 5′ and the 3′ homologous region, respectively, of the targeting vector. A LoxP site was generated by oligo synthesis (Operon, Huntsville, AL) and was inserted into the junction between the 5′ homologous region and the *Avr*II-*Afl*II genomic fragment containing exon 4. A second LoxP site was introduced from 1 of 2 LoxP sites in the Neo(LoxP) cassette (Figure 1A). The targeting vector was linearized with *Not*I and electroporated into J1 ES cells, and *Runx1*$^{tm3Spe/+}$ (*Runx1*$^{F/+}$) F1 mice were generated by standard protocols. The 5′ and 3′ targeting probes were used to screen for homologous recombination events and to confirm the correct targeting. The 5′ probe recognizes a 7.3-kb *Bam*HI fragment in the wild-type *Runx1* allele and a 4.7-kb *Bam*HI fragment in the targeted allele. The 3′ probe recognizes an 11.5-kb *Ssp*I fragment in the wild-type allele and a 13.5-kb fragment in the targeted allele (Figure 1A).

Runx1$^{F/F}$ and *Runx1*$^{F/F}$—Tg(*Mx1*-Cre) colony generation

All mice were housed in a pathogen-free animal facility in microisolator cages. *Runx1*$^{F/+}$ mice were backcrossed against C57BL/6 mice (Taconic, Germantown, NY) for 3 generations, then intercrossed to obtain *Runx1*$^{F/F}$ mice. Tg(*Mx1* [myxovirus resistance 1 gene]–Cre) mice[49] were similarly backcrossed onto C57BL/6. *Runx1*$^{F/F}$ mice were mated to *Runx1*$^{+/+}$—Tg(*Mx1*-Cre) mice to generate *Runx1*$^{F/+}$—Tg(*Mx1*-Cre) mice. *Runx1*$^{F/+}$—Tg(*Mx1*-Cre) mice were mated to *Runx1*$^{F/F}$ mice to generate *Runx1*$^{F/F}$—Tg(*Mx1*-Cre) mice. *Runx1*$^{F/F}$—Tg(*Mx1*-Cre) mice were mated to *Runx1*$^{F/F}$ mice to generate *Runx1*$^{F/F}$—Tg(*Mx1*-Cre) and *Runx1*$^{F/F}$ littermates for phenotypic analysis. To evaluate the *Runx1*^{F} allele in the *Runx1* null (designated *Runx1*^{tm1Spe} or *Runx1*rd) background,[11] *Runx1*$^{F/F}$—Tg(*Mx1*-Cre) mice were crossed to *Runx1*$^{+/rd}$ mice backcrossed 7 generations onto BALB/c (Taconic) to generate CXB6F1 *Runx1*$^{F/rd}$—Tg(*Mx1*-Cre) mice and littermate controls (*Runx1*$^{F/rd}$, *Runx1*$^{F/+}$—Tg(*Mx1*-Cre), and *Runx1*$^{F/+}$). In *Runx1*$^{F/rd}$—Tg(*Mx1*-Cre) mice, a single *Runx1* Cre-mediated excision event results in a *Runx1* null genotype.

Tail genomic DNA was obtained using a Puregene DNA isolation kit (Gentra Systems, Minneapolis, MN). Mice were genotyped for the *Runx1*^{F}

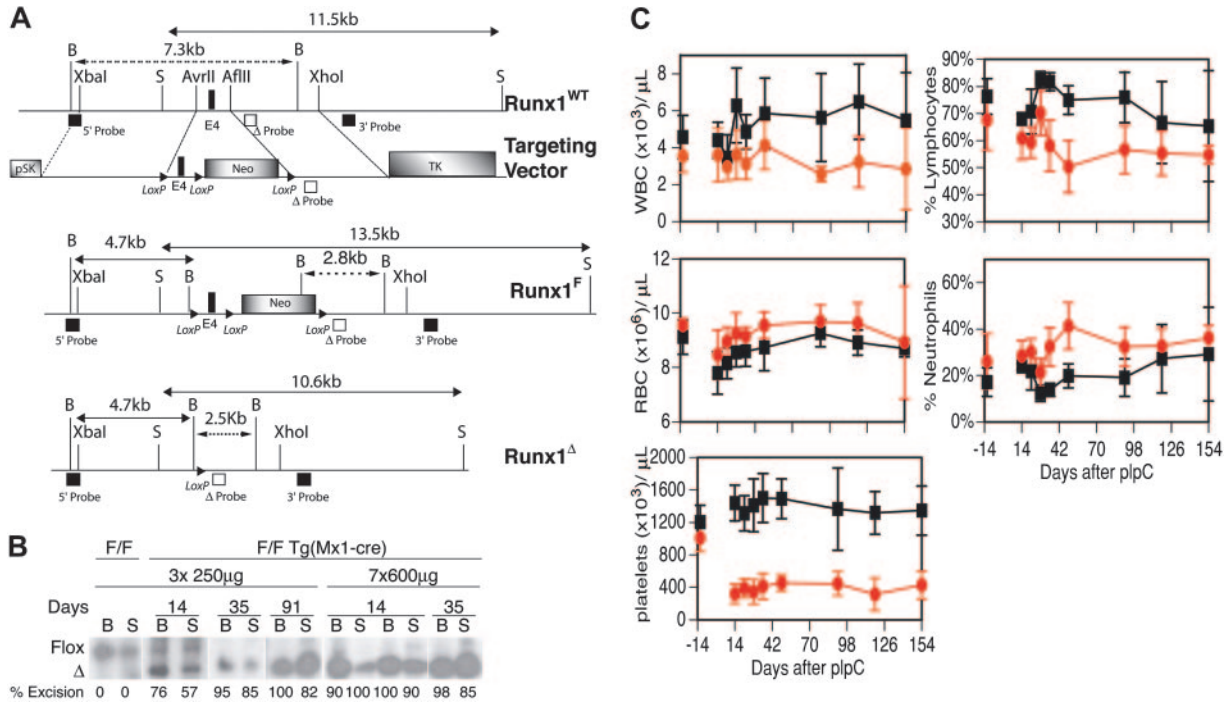

Figure 1. Inducible *Runx1* excision in adult mice induces thrombocytopenia. (A) Schematic representation of *Runx1* gene-targeting strategy used to flank exon 4 with LoxP-targeting sites. B indicates *Bam*HI; S, SspI; E4, Runt domain exon 4. (filled boxes) 5′ and 3′ targeting probes. (dashed arrows) *Bam*HI-digested genomic DNA fragments for wild-type (7.3-kb), Floxed (2.8-kb), and excised (2.5-kb) DNA detected with excision (Δ) probe (open boxes) located 3′ to the distal LoxP site. (B) Southern blot analysis of *Bam*HI-digested genomic DNA from bone marrow [B] and spleen [S] cells of representative mice killed at 14, 35, and 91 days after pIpC injection. The dose of pIpC is indicated. The blots are probed with Δ probe, which detects the Floxed (2.8-kb) and excised (2.5-kb) *Runx1* alleles. Numbers indicate percentage excision. (C) Mean ± SD of total WBC counts, total red blood cell (RBC) counts, total platelet counts, percentage lymphocytes, and percentage neutrophils in PB of pIpC-treated *Runx1*$^{F/F}$—Tg(*Mx1*-Cre) (red symbols) and *Runx1*$^{F/F}$ (black symbols) mice. Mice were bled 12 days before pIpC injection and 14, 21, 28, 35, 49, 91, 119, and 154 days after pIpC injection. The number of animals evaluated for each genotype at the respective time points is N (*Runx1*$^{F/F}$—Tg(*Mx1*-Cre) = 14, 14, 12, 8, 10, 9, 8, 7 and 6; N (*Runx1*$^{F/F}$) = 7, 5, 7, 7, 5, 7, 6, 6, and 6.

allele by polymerase chain reaction (PCR). Reactions (20 μL) were performed with 80 μM forward (Rdintron 5′, GAGTCCCAGCTGTCAATTCC 3′) and reverse (Rdexon4 5′, GGTGATGGTCAGAGTGAAGC 3′) primers, 250 μM dNTPs, 1.5 mM $MgCl_2$, 2.5 U *Taq* (Invitrogen) and 5 to 50 ng DNA. DNA was denatured at 94°C for 3 minutes, then amplified by 40 cycles at 94°C for 30 seconds, 60°C for 1 minute, and 72°C for 1 minute. *Runx1*rd alleles were similarly genotyped with Rdintron and RD29 (5′) TCGCAGCGCATCGCCTTCTA 3′). The *Mx1*-Cre genotype was performed by Southern blot analysis of *Bam*HI-digested genomic tail DNA.

Induction of *Mx1*-Cre expression and *Runx1*$^{F/F}$ excision in adult mice

Eight- to 12-week-old mice were injected intraperitoneally with sterile polyinosinic-polycytidylic acid (pIpC) (Sigma, St Louis, MO) dissolved at 2 mg/mL in phosphate-buffered saline (PBS; Invitrogen, Carlsbad, CA). One cohort of mice (3 *Runx1*$^{F/F}$ and 4 *Runx1*$^{F/F}$—Tg(*Mx1*-Cre)) was injected every other day for 3 injections with 125 μL (250 μg/dose).[49] *Runx1*^{F} excision was variable with this dose (Figure 1B). Therefore, all studies were performed with mice receiving 7 injections, every other day, of 300 μL (600 μg/dose).[46] All times after pIpC induction are counted from the first day of injection (day 0). Mice were anesthetized with methoxyflurane or isoflurane according to institutional guidelines (Harvard University, Boston, MA) and retro-orbital eye bleeds were performed. Automated cell counts were performed at Children's Hospital (Boston, MA) using murine-specific software.

Runx1$^{F/F}$ excision evaluation

Excision of floxed *Runx1* alleles after Cre expression was evaluated using Southern blot or PCR analysis. Single-cell suspensions of bone marrow (BM), spleen, or thymus cells were prepared as described previously.[50,51] Genomic DNA (10-20 μg) was digested with *Bam*HI, separated in 0.7% agarose gel, and transferred to Hybond-N+ membranes (Amersham Biosciences, Piscataway, NJ). The excision (Δ) probe (Figure 1A) is located within *Runx1* intron 4, 3′ to the most distal LoxP site, and hybridizes to *Runx1*$^{+}$ (7.3 kb), *Runx1*^{F} (2.8 kb), and *Runx1*$^{F\text{-}Excised}$ (designated *Runx1*$^{\Delta}$) (2.5 kb) genomic DNA (Figure 1A-B) but not to *Runx1*rd. Probe template DNA was generated in PCR with the primers RX1FldelF (5′) TGCGCTTACAGAATGTCAGG (3′) and RX1FldelR (5′) CATGACCATGATTGCAGGAG 3′. Alternatively, excision was evaluated by 3-primer PCR, performed as described earlier in this paragraph with 80 μM Rdintron and 40 μM each of Rdexon4 and LoxPrev113 (5′) CCAAGATAGTCCTTAACGGTCG 3′).

Histopathology

Histopathologic examination was conducted as previously described.[51] Critical analyses were performed by a hematopathologist blinded to genotype (J.L.K.). Histologic images were obtained on a Nikon Eclipse E400 microscope (Nikon, Tokyo, Japan) equipped with a SPOT RT color digital camera model 2.1.1 (Diagnostic Instruments, Sterling Heights, MI). The microscope was equipped with a 10×/22 ocular lens. Low power images (×100) were obtained with a 10×/0.25 objective lens. High power images (×600) were obtained with a 60×/1.4 objective lens with oil (Trak 300; Richard Allan Scientific, Kalamazoo, MI). Images were cropped in Adobe Photoshop 6.0 (Adobe Systems, San Jose, CA) and composed in Adobe Illustrator for CS (Adobe Systems).

In vitro colony assays

Myeloid colony-plating assays were performed in methylcellulose-based medium (M3434) containing 3 U/mL erythropoietin (EPO), 10 ng/mL recombinant murine interleukin-3 (rmIL-3), 10 ng/mL rmIL-6, and 50 ng/mL recombinant murine stem cell factor (rmSCF), as per the manufacturer's protocols (StemCell Technologies, Vancouver, BC, Canada). Cells were plated in 3 dilutions (2×10^4, 1×10^4, 5×10^3 cells/dish) in duplicate and were incubated for 12 days at 37°C. Colonies were counted at dilutions in which 30 to 60 colonies per plate were observed. Similar plating efficiencies were observed with fresh and previously frozen BM cells. Colonies were scored by morphology and Wright-Giemsa–stained slides of cytospins. Individual colonies were washed and suspended in 200 μL PBS. One hundred microliters of this suspension was plated on slides with a Cytospin4 centrifuge (Thermo Shandon, Pittsburgh, PA) for 5 minutes at 36*g*. The remaining cells were suspended in 50 μL water and boiled for 5 minutes, and 5 μL was used in a PCR. Megakaryocyte plating assays were performed in collagen-containing medium according to the manufacturer's protocol (MegaCult-C; StemCell Technologies). Slides were fixed and stained for 6 hours with acetylcholine iodide (Sigma, St Louis, MO), as per the MegaCult-C protocol, and were counterstained with Harris hematoxylin solution (Sigma).

Bone marrow transplantation

Single-cell suspensions of BM cells were prepared as described previously.[50,51] Cells were stored in 90% fetal calf serum and 10% dimethyl sulfoxide (DMSO; Sigma) in liquid nitrogen. Cells were thawed at 37°C and washed in PBS, and viable cells were counted by trypan blue dye exclusion (Sigma). Thawed cells consistently demonstrated viability of 40% to 50% after thawing (trypan blue dye exclusion). For competitive repopulation assays, competitor BM was obtained from wild-type B6.SJL (CD45.1^{+}) mice (Jackson Laboratories, Bar Harbor, ME) on the day of transplantation. Total (6×10^5) viable BM cells (0.6 mL) at a test-competitor ratio of 4:1 were injected into the lateral tail veins of lethally irradiated (2×650 cGy) female recipient B6.SJL mice. Blood was obtained by retro-orbital bleeding at 4, 8, and 19 weeks after transplantation for flow cytometric analysis. For noncompetitive transplantations, 1×10^6 total BM cells in 0.6 mL were injected. Mice were housed in microisolator cages with autoclaved chow and acidified water.

Flow cytometric analysis

Sorting of myeloid progenitors was accomplished by staining BM cells from mice 17 weeks (fresh) or 27 and 39 weeks (frozen) after pIpC induction with purified rat anti–IL-7Rα chain monoclonal antibodies (A7R34) (e-Bioscience, San Diego, CA) and purified or phycoerythrin (PE)–Cy5-conjugated rat antibodies specific for the following lineage markers: CD3 (CT-CD3), CD4 (RM4-5), CD8 (5H10), B220 (6B2), Gr-1 (8C5), Ter119, and CD19 (6D5) (Caltag, Burlingame, CA). IL-7Rα^{+}Lin^{+} cells were removed with sheep anti–rat immunoglobulin G (IgG)–conjugated magnetic beads (Dynabeads M-450; Dynal A.S., Oslo, Norway), and the remaining cells were stained with PE-Cy5–conjugated goat anti–rat IgG (Caltag). Cells were then stained with R-phycoerythrin (PE)–conjugated anti–FcγRII/III (2.4G2), fluorescein-isothiocyanate (FITC-)–conjugated anti–CD34 (RAM34), allophycocyanin (APC)–conjugated anti–c-Kit (2B8), and biotinylated anti–Sca-1 (E13-161-7) monoclonal antibodies (BD PharMingen, San Diego, CA), followed by avidin-APC-Cy7 (Caltag). Myeloid progenitors were sorted as IL-7Rα^{-}Lin^{-}Sca-1^{-}c-Kit^{+}CD34^{+}FcγRII/III^{lo} (common myeloid progenitor [CMP]), IL-7Rα^{-}Lin^{-}Sca-1^{-}c-Kit^{+}CD34^{+}FcγRII/III^{hi} (granulocyte-monocyte progenitor [GMP]), and as IL-7Rα^{-}Lin^{-}Sca-1^{-}c-Kit^{+}CD34^{-}FcγRII/III^{lo} megakaryocyte-erythrocyte progenitor [MEPs], as described previously.[52] Hematopoietic stem cells (HSCs) and common lymphocyte progenitor cells (CLPs) were sorted as IL-7Rα^{-}Lin^{-}Sca-1^{hi}c-Kit^{hi} and IL-7Rα^{+}Lin^{-}Sca-1^{lo}c-Kit^{lo} populations, respectively.[53]

Additional flow cytometric analysis was performed on a 4-color FACScalibur cytometer (Becton Dickinson, Mountain View, CA) and analyzed using CellQuest software. All antibodies were obtained from BD PharMingen. Cells were preincubated with 1 μg purified rat anti–mouse CD16/CD32 before staining. Competitive reconstitution was assayed by staining 250 μL fresh red blood cell–lysed peripheral blood (PB) with 1 μg fluorescein isothiocyanate (FITC)–mouse anti–mouse CD45.1 and 1 μg PerCP-Cy5.5 mouse anti–mouse CD45.2 of scatter-gated nucleated cells. Additional flow cytometric analyses were performed on previously frozen cell suspensions. Double-negative (DN) thymocytes were stained with FITC-rat anti–mouse CD8a and PerCP–Cy5.5-rat anti–mouse CD4 or with FITC-anti–CD45.1, PerCP–Cy5.5-rat anti–mouse CD4, PerCP–Cy5.5-rat anti–mouse CD8a, PE-rat anti–mouse CD44, and APC-rat anti–mouse CD25. CD25 and CD44 stainings were evaluated in CD45^{+}CD4^{-}CD8^{-} gated cells. The percentage of myeloid cells in spleen and BM was

determined by staining with FITC–anti-CD45.2, PE–rat anti–mouse CD11b (Mac-1), 7AAD-PerCP-Cy5.5 (for viability), and APC–rat anti–mouse Ly-6G and Ly-6C (Gr-1) or PE–rat anti–mouse c-KIT and APC–rat anti–mouse Ter119. Freshly derived BM cells from 2 femurs and 2 tibias were cultured in Dulbecco modified Eagle medium (DMEM) + 10% fetal calf serum with 10 ng/mL recombinant murine thrombopoietin (rmTPO; Sigma) and 50 ng/mL rhIL-11 (StemCell Technologies) for 4 days before flow cytometric analysis of DNA content. BM megakaryocytes were stained with FITC–rat anti–mouse CD41, followed by 50 μg/mL propidium iodide in 0.1% sodium citrate buffer and then incubated with 50 μg/mL RNAase (Qiagen, Valencia, CA), as previously described.[54]

Results

Excision of a conditional *Runx1* allele in adult hematopoietic tissues

To test the effects of loss of *Runx1* on adult hematopoietic tissues, we constructed a conditional knock-out allele of the *Runx1* locus in mice that could be inactivated using the Cre-LoxP conditional targeting system (Figure 1A). This allows for tissue-specific deletion of a LoxP-flanked (floxed) exon of *Runx1* after tissue-specific expression of Cre recombinase. Excision of the floxed *Runx1* allele (*Runx1*^{tm3Spe}, *Runx1*^{F}) by the early embryonic Cre deleter strain Tg(*EIIa*-Cre)[55] recapitulated the embryonic lethal phenotype associated with homozygosity for a previously derived *Runx1* allele (*Runx1*rd), in which neo replaces exon 4[11] (data not shown). In transgenic (Tg) *Mx1*-Cre mice, the interferon-inducible promoter *Mx1* allows for expression of Cre recombinase in the hematopoietic system in response to interferon or interferon-inducing agents such as pIpC.[49] *Runx1*$^{F/F}$ and *Runx1*$^{F/F}$—Tg(*Mx1*-Cre) littermates on the C57BL/6 background were induced for excision at 8 to 12 weeks of age by intraperitoneal injection of pIpC, and PB counts were monitored for 22 weeks. We compared 2 pIpC dosing regimens, 3 doses of 250 μg every other day and 7 doses of 600 μg every other day. The latter dosing regimen induced a more than 90% excision of the *Runx1*^{F} allele throughout the observation period, as demonstrated by Southern blot analysis, and was subsequently used for all further studies (Figure 1B; data not shown). Although *Runx1* is essential for the establishment of definitive hematopoiesis during development, we observed, as did Ichikawa et al,[56] that adult hematopoietic development was maintained after the excision of *Runx1*^{F} (Figure 1C). There were, however, several distinctive hematopoietic abnormalities affecting all lineages. Within this cohort of mice, these findings included an average approximately 80% decrease in platelets, an approximately 39% decrease in total white blood cell (WBC) counts, an approximately 22% decrease in the percentage of lymphocytes, and an approximately 28% increase in the percentage of neutrophils during the course of the observation period. We made similar observations after *Runx1* excision in *Runx1*$^{F/rd}$—Tg(*Mx1*-Cre) mice on a C57BL/6 × BALB/c F1 (C×B6F1) background (data not shown). PB counts of *Runx1* heterozygous mice (*Runx1*$^{F/rd}$ and *Runx1*$^{F/+}$—Tg(*Mx1*-Cre) were not significantly different from *Runx1*$^{F/+}$ mice (data not shown).

Effects of *Runx1* excision on the hematopoietic stem cell compartment

Because *Runx1* is essential for definitive hematopoiesis during development, we first assayed for the presence of HSCs in *Runx1*-deficient animals by enumerating the IL-7Rα^{-}Lin^{-}Sca-1^{hi}c-Kit^{hi} population in total BM. The percentage of phenotypically defined HSCs was increased approximately 3-fold ($P = .011$) after *Runx1*^{F} excision by *Mx1*-Cre (Table 1). This increase in HSCs was observed at 17, 27, and 39 weeks after pIpC, indicating that *Runx1* is not required to maintain a phenotypic HSC compartment in adult mice. PCR analysis showed complete excision in the HSC compartment (Figure 2A).

We next evaluated stem cell function by testing the ability of *Mx1*-Cre–excised *Runx1* BM to competitively repopulate the adult hematopoietic compartment in lethally irradiated syngeneic mice. BM from a pIpC-treated *Runx1*$^{F/F}$—Tg(*Mx1*-Cre) (CD45.2^{+}) mouse or a control pIpC-treated *Runx1*$^{F/F}$ (CD45.2^{+}) mouse was transplanted into lethally irradiated congenic B6.SJL (CD45.1^{+}) mice with wild-type competitor B6.SJL (CD45.1^{+}) BM (4:1 ratio of test cells to competitor cells). Mice were monitored for contributions of CD45.2^{+} donor cells to PB at 4, 8, and 19 weeks after transplantation (Figure 2B).[57] Control *Runx1*$^{F/F}$ donor BM reconstituted B6.SJL recipients in all animals tested (n = 6), with contributions from the CD45.2^{+} donor cells increasing with time after transplantation (Figure 2C). The average contribution of *Runx1*$^{F/F}$ BM to total PB WBCs at 19 weeks after transplantation was 54.5%. BM from *Mx1*-Cre excised *Runx1*$^{F/F}$ mice also contributed to hematopoietic reconstitution at all time points, but reconstitution decreased with time. Two of 8 animals failed to show reconstitution at any time point. At 19 weeks after transplantation, *Mx1*-Cre–excised CD45.2^{+} donor cells (n = 6) accounted for an average of 10% of total PB WBCs. Three of 8 mice demonstrated significant contributions (3%, 17%, and 39%) to PB (not shown) at 19 weeks after transplantation. PCR of *Runx1* loci from BM confirmed these findings (Figure 2D), indicating that *Runx1*-excised marrow has reduced competitive repopulating ability in assays for long-term repopulating activity.

We next tested whether *Runx1*-excised BM could repopulate syngeneic B6.SJL (CD45.1^{+}) mice in the absence of competitor BM. Lethally irradiated B6.SJL (CD45.1^{+}) mice underwent transplantation with 1 × 10^{6} BM cells from a pIpC-treated *Runx1*$^{F/F}$—Tg(*Mx1*-Cre) (CD45.2^{+}) mouse or a control pIpC-treated *Runx1*$^{F/F}$

Table 1. Stem and progenitor cell populations in *Runx1*$^{F/F}$—Tg(*Mx1*-Cre) BM

		Genotype					
		Runx1$^{F/F}$		*Runx1*$^{F/F}$—Tg(*Mx1*-Cre)			
Cell type	Marker content	BM, %, mean ± SD*	No. mice	BM, %, mean ± SD*	No. mice	Fold change	*P*†
HSC	IL-7Rα^{-}Lin^{-}Sca-1^{hi} c-Kit^{hi}	0.34 ± 0.1	4	0.99 ± 0.5	6	2.9	.011
CLP	IL-7Rα^{+}Lin^{-}Sca-1^{lo} c-Kit^{lo}	0.07 ± 0.01	4	<0.01 ± <0.01	6	>−7.0	.019
CMP	IL-7Rα^{-}Lin^{-}Sca-1^{-} c-Kit^{+} CD34^{+} FcγRII/III^{+}	0.37 ± 0.1	3	0.30 ± 0.2	4	−0.8	.377‡
GMP	IL-7Rα^{-}Lin^{-}Sca-1^{-} c-Kit^{+} CD34^{+} FcγRII/III^{hi}	0.67 ± 0.1	3	1.98 ± 0.8	4	3.0	.032

*Percentage of total BM. Detection limit is 0.01%. Data are results from 17, 27, and 39 weeks after pIpC.
†Mann-Whitney *U* test.
‡Not statistically different.

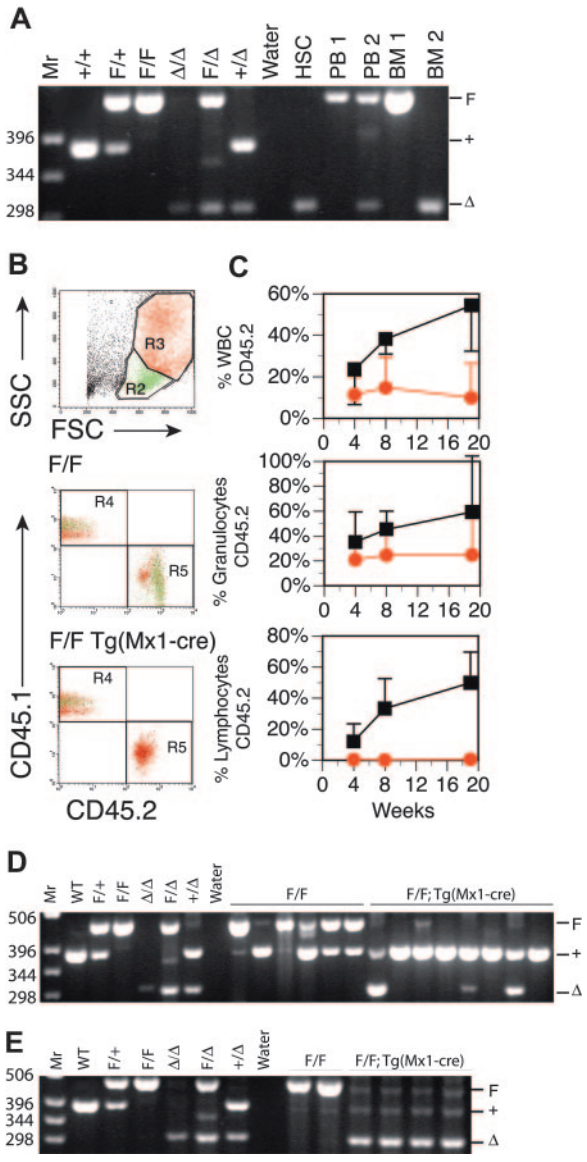

Figure 2. Stem cells from pIpC-treated *Runx1*$^{F/F}$—Tg(*Mx1*-Cre) mice are reduced in competitive repopulation ability. (A) Ethidium bromide (EtBr)–stained 3% agarose gel of 3-primer PCR of *Runx1* loci from sorted HSCs derived from fresh BM 17 weeks after pIpC (Table 1) and unfractionated BM and PB. 1 = *Runx1*$^{F/F}$; 2 = *Runx* $^{F/F}$—Tg(*Mx1*-Cre). Mr = 1-kb ladder, sizes indicated (bp). Control samples include tail DNA from *Runx1*$^{+/+}$, *Runx1*$^{F/+}$, and *Runx1*$^{F/F}$ mice and from *Runx1*$^{Δ/Δ}$, *Runx1*$^{F/Δ}$, and *Runx1*$^{+/Δ}$ embryos. *Runx1*^{Δ} alleles were generated by mating *Runx1*$^{F/F}$ mice to Tg(EIIa-Cre) mice and intercrossing *Runx1*$^{F/Δ}$ mice. (B) Composite showing gating strategy and CD45.1/CD45.2 staining of PB from representative mice that underwent transplantation with *Runx1*$^{F/F}$ or *Runx1*$^{F/F}$—Tg(*Mx1*-Cre) and competitor marrow 8 weeks after transplantation. Green indicates lymphocytic (R2), and red indicates granulocytic (R3) fractions based on scatter gating (SSC, side scatter; FSC, forward scatter). Gate assignments were confirmed by back-gating of control stainings with Gr1^{+}–, Mac1^{+}–, CD3^{+}–, T-cell receptor β (TCRβ^{+})–, CD19^{+}–, or B220^{+}–stained PB (not shown). The percentage contribution to the granulocytic and lymphocytic lineages of PB from each marrow isotype (CD45.1/CD45.2) was determined. (C) Plotted is the mean (±SD) percentage contribution of donor-derived CD45.2^{+} cells in PB from mice that underwent transplantation with *Runx1*$^{F/F}$—Tg(*Mx1*-Cre) (red symbols; n = 6) or *Runx1*$^{F/F}$ (black symbols; n = 6) and competitor bone marrow to total WBCs, granulocytes, and lymphocytes of recipient mice at 4, 8, and 19 weeks after transplantation. Two of 8 mice receiving *Runx1*$^{F/F}$—Tg(*Mx1*-Cre) marrow that failed to show contribution of CD45.2^{+} marrow to PB of recipient mice at any time point are excluded. (D) Nineteen weeks after transplantation, EtBr-stained 3% agarose gel of 3-primer PCR of *Runx1* loci of BM from mice that underwent competitive transplantation. (E) EtBr-stained 3% agarose gel of 3-primer PCR of *Runx1* loci from BM of mice that underwent transplantation without competitor marrow.

Table 2. Hematopoietic effects of *Runx1* excision are transplantable

PB counts†	Donor cell genotype*	
	Runx1$^{F/F}$, mean ± SD	*Runx1*$^{F/F}$-Tg(Mx1-Cre), mean ± SD
WBCs, ×10^3/μL	6.94 ± 2.3	3.55 ± 0.4
RBCs, ×10^6/μL	7.53 ± 1.7	9.46 ± 0.5
Platelets, ×10^3/μL	1808 ± 200	364 ± 140
Neutrophils, %	32.9 ± 4.6	40.6 ± 2.6
Lymphocytes, %	60.0 ± 4.6	49.0 ± 3.1
Lineage and origin of PB cells‡		
WBC donor derived, CD45.2^{+}, %§	98.7 ± 0.5	87.9 ± 3.4
PB T cells		
CD3^{+} %‖	3.6 ± 1.8	9.0 ± 1.7
CD3^{+} donor derived, %¶	70.9 ± 22.0	7.0 ± 4.5
PB B cells		
B220^{+}, %‖	35.4 ± 7.3	0.6 ± 0.3
B220^{+} donor derived, %¶	100.0 ± 0.0	97.1 ± 4.5
PB myeloid cells		
Mac1^{+}, %‖	6.4 ± 2.1	17.1 ± 3.7
Mac1^{+} donor derived, %¶	99.6 ± 0.2	99.1 ± 0.4
Gr1^{+}/Mac1^{+}, %‖	40.5 ± 71.2	67.8 ± 32.9
Gr1^{+}/Mac1^{+} donor derived, %¶	99.8 ± 0.3	98.1 ± 0.8
Gr1^{+}, %‖	1.0 ± 0.4	9.8 ± 1.3
Gr1^{+} donor derived, %¶	45.5 ± 34.7	4.9 ± 1.7

Results are for 2 *Runx1*$^{F/F}$ mice (2 others were lost to fighting) and 4 *Runx1*$^{F/F}$-Tg(*Mx1*-Cre) mice.

*Genotypes of donor cells (CD45.2^{+}) transplanted into lethally irradiated B6.SJL (CD45.1^{+}) recipient mice. Mice were killed 14 weeks after transplantation.

†Results from automated blood counts.

‡Cells gated by scatter, CD45.1, and CD45.2.

§Indicated is the percentage of total WBCs (pan-CD45^{+}) that were donor derived (CD45.1^{-} and CD45.2^{+}).

‖Indicated is the percentage of total WBCs (pan-CD45^{+}) that were CD3, B220, Mac-1, or Gr-1 positive.

¶Indicated is the percentage of total CD3-, B220-, Mac-1-, Mac-1/Gr-1-, or Gr-1-positive WBCs (pan-CD45^{+}) that were donor derived (CD45.2^{+}).

(CD45.2^{+}) mouse. Mice receiving *Runx1*$^{F/F}$—Tg(*Mx1*-Cre) marrow (n = 4) were viable at 14 weeks after transplantation, indicating that *Runx1*-excised cells are competent for reconstitution (Figure 2E). The alterations in PB counts observed in primary animals (Figure 1C), including an 80% decrease in platelet counts, 49% decrease in WBC counts, and relative changes in the differential, were observed in mice that underwent transplantation with excised *Runx1*$^{F/F}$—Tg(*Mx1*-Cre) BM. (Table 2). In nonexcised recipients, approximately 1.3% of the PB cells were derived from the host (CD45.1^{+}), whereas approximately 12.1% of the PB cells in excised recipients were derived from the host (Table 2). Thus, even under these stringent selective conditions for HSC repopulation, *Runx1*-excised HSCs are less competitive under repopulating conditions than wild-type HSCs.

Effects of *Runx1* excision on the lymphoid lineage

Mature B and T cells were present in pIpC-treated *Runx1*$^{F/F}$—Tg(*Mx1*-Cre) mice, but the lymphocyte count in PB was reduced by an average of approximately 50% (Figure 1C). There was an average 19.7-fold (P = .007) reduction in the percentage of mature B cells (CD19^{+}B220^{+}) in the BM of excised mice (Figure 3A). Pre-B (IgM^{-}NK1.1^{-}Lin^{-}CD43^{-}B220^{+}) and pro-B (IgM^{-}NK1.1^{-}Lin^{-}CD43^{+}B220^{+}) cell precursors were nearly undetectable (less than 0.1%) in excised mice (Figure 3A), consistent with an early block in B-cell maturation.

There were also marked defects in T-lineage development in *Mx1*-Cre–excised *Runx1* animals. The total cellularity of the

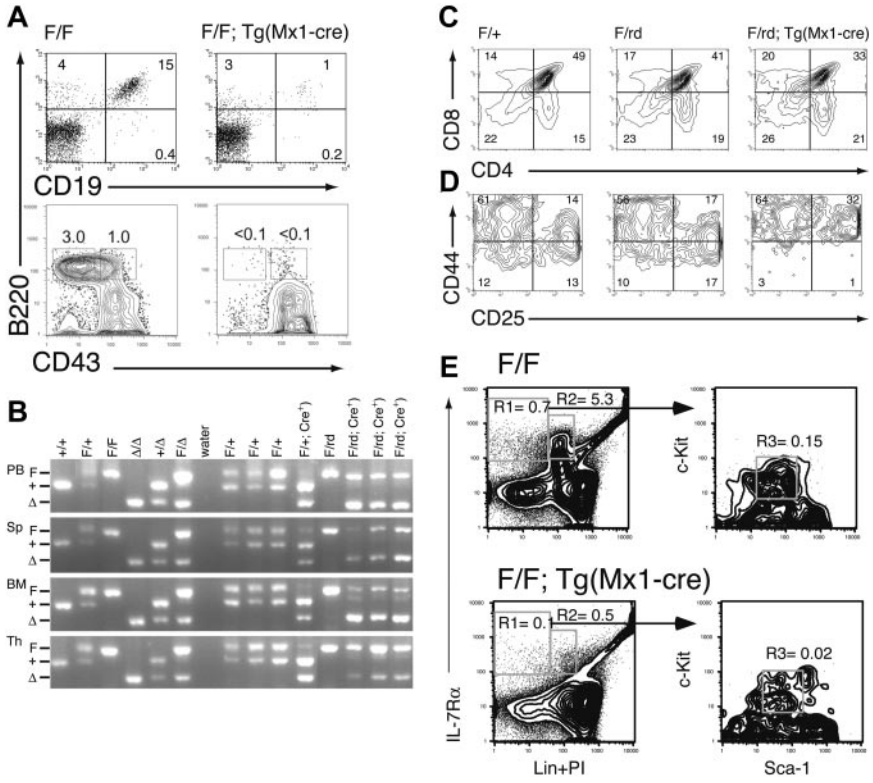

Figure 3. Lymphoid development is inhibited in *Runx1*-excised mice. (A) Representative B220/CD19 and B220/CD43 staining of BM from *Runx1*$^{F/F}$ and *Runx1*$^{F/F}$—Tg(*Mx1*-Cre) mice. CD43 staining is shown for cells gated as IgM$^-$NKK1.1$^-$Lin$^-$. Numbers indicate percentage of cells gated in each respective quadrant. (B) EtBr-stained 3% agarose gels with 3-primer PCR products of *Runx1* loci in PB, spleen (Sp), BM, and thymocytes (Th) of mice 154 days after pIpC. Genotypes are as indicated. Control samples are as in Figure 2. The primers do not amplify a product from the *Runx1*rd allele. (C) Shown are CD4 and CD8 staining from representative animals of genotypes, *Runx1* $^{F/+}$, *Runx1*$^{F/rd}$, and *Runx1*$^{F/rd}$—Tg(*Mx1*-Cre). Numbers indicate percentage of cells gated in each respective quadrant. (D) Shown are CD25 and CD44 staining of CD45.2$^+$CD4$^-$CD8$^-$ gated thymocytes from representative animals, as in panel C. (E) Composite of high-speed flow cytometric analysis of BM from representative *Runx1*$^{F/F}$ and *Runx1*$^{F/F}$—Tg(*Mx1*-Cre) mice. Numbers indicate percentages of total BM for indicated populations. Gated populations indicated include IL-7Rα$^+$Lin$^-$ (R1), IL-7Rα$^+$Lin$^+$ (R2) (which includes immature B cells), and CLP (R3), as indicated in Table 1. PI indicates propidium iodide.

thymus was reduced approximately 10-fold compared with littermate controls (not shown). Although there was 90% or greater excision of *Runx1*^{F} allele in BM, the percentage of excised alleles was 50% or less in thymocytes from either *Runx1*$^{F/F}$—Tg(*Mx1*-Cre) (not shown) or *Runx1*$^{F/rd}$—Tg(*Mx1*-Cre) mice (Figure 3B). This suggests that *Mx1*-Cre expression in the thymus is lower than in BM. To distinguish between the effects of homozygous and heterozygous excision, we evaluated thymic T-cell maturation in *Runx1*$^{F/rd}$—Tg(*Mx1*-Cre) (CXB6F1) and littermate mice. There was a 37% decrease ($P = .033$) in the relative percentage of CD4$^+$CD8$^+$ (double-positive [DP]) thymocytes in *Mx1*-Cre excised *Runx1*$^{F/rd}$ mice compared with *Runx1*$^{F/+}$ mice (Figure 3C). We did not observe a significant expansion of the CD4$^-$CD8$^-$ (DN) population. However, this was likely obscured by the approximately 40% increase ($P = .024$) in CD4$^+$CD8$^-$ (SP4) cells compared with *Runx1*$^{F/+}$ mice. This increase in SP4 cells likely resulted from the requirement for *Runx1* repression of CD4 expression during thymocyte maturation from the DN to the DP stage.[6,7] There was an approximate 3-fold decrease in the percentages of DN3 (CD44$^-$CD25$^+$) ($P = .033$) and DN4 (CD44$^-$CD25$^-$) ($P = .011$) cells relative to *Runx1*$^{F/+}$ thymocytes (Figure 3D). Relative to *Runx1*$^{F/rd}$ and *Runx1*$^{F/+}$—Tg(*Mx1*-Cre) mice, the percentage of DN3 and DN4 cells were reduced 4.3-fold ($P = .018$) and 2.3-fold ($P = .018$) in *Runx1*$^{F/rd}$—Tg(*Mx1*-Cre) mice, respectively.

To determine the earliest step in lymphocyte development requiring *Runx1*, we enumerated the number of BM-derived CLPs (IL-7Rα$^+$Lin$^-$Sca-1^{lo}c-Kit^{lo}) in *Runx1*$^{F/F}$—Tg(*Mx1*-Cre)–excised mice. This revealed a greater than 7-fold decrease ($P = .019$) in the percentage of CLPs in the BM of *Runx1*-excised mice (Figure 3E; Table 1). We next evaluated lymphocyte commitment in mice after transplantation. In the competitive reconstitution assay, there was a complete lack of contribution of excised *Runx1*$^{F/F}$—Tg(*Mx1*-Cre) donor cells to the lymphocyte lineages (Figure 2C). In noncompetitive repopulation assays, *Runx1*$^{F/F}$—Tg(*Mx1*-Cre) contributed to T- and B-cell lineages to a limited extent (Table 2). The percentage of CD3$^+$ T cells in *Runx1*-excised recipients was increased 2.5-fold compared with nonexcised recipients. However, 93% of CD3$^+$ T cells were derived from the host BM (CD45.1$^+$). Strikingly, peripheral blood B220$^+$ B cells were decreased 58-fold in excised recipients compared with nonexcised recipients. In contrast to the T-cell lineage, 97% of PB B cells were donor derived. Together, these findings suggest that *Runx1* is not required for lymphocyte maturation but that the loss of *Runx1* inhibits lymphocyte maturation at early and late stages of development.

Effects of *Runx1* excision on the myeloid lineage

The marked defects in lymphocyte maturation observed in *Runx1*-excised mice are sharply contrasted with the effects of *Runx1* excision on the myeloid lineage. All myeloid lineages, including granulocytes, monocytes, erythrocytes, and platelets, were represented in *Mx1*-Cre–excised *Runx1*$^{F/F}$ (Figure 1C) and *Runx1*$^{F/rd}$ (data not shown) animals. No significant abnormalities were observed in the erythroid lineage. However, we observed significant defects in the megakaryocytic lineage. Although there was no clinically evident bleeding diathesis, within 14 days of pIpC injection there was an approximately 80% reduction in average PB platelet counts in *Runx1*$^{F/F}$—Tg(*Mx1*-Cre) (Figure 1C) and *Runx1*$^{F/rd}$—Tg(*Mx1*-Cre) (not shown) mice compared with littermate controls. Histologic examination of BM from pIpC-treated *Runx1*$^{F/F}$—Tg(*Mx1*-Cre) (Figure 4A-B) and *Runx1*$^{F/rd}$—Tg(*Mx1*-Cre) (not shown) mice showed a marked decrease in the number of mature megakaryocytes compared with control mice, suggesting that the decrement in platelet count was attributed to decreased megakaryocyte maturation. This defect was observed in animals that underwent transplantation, indicating that the megakaryocyte maturation defect is cell autonomous (Figure 4C). Propidium iodide staining

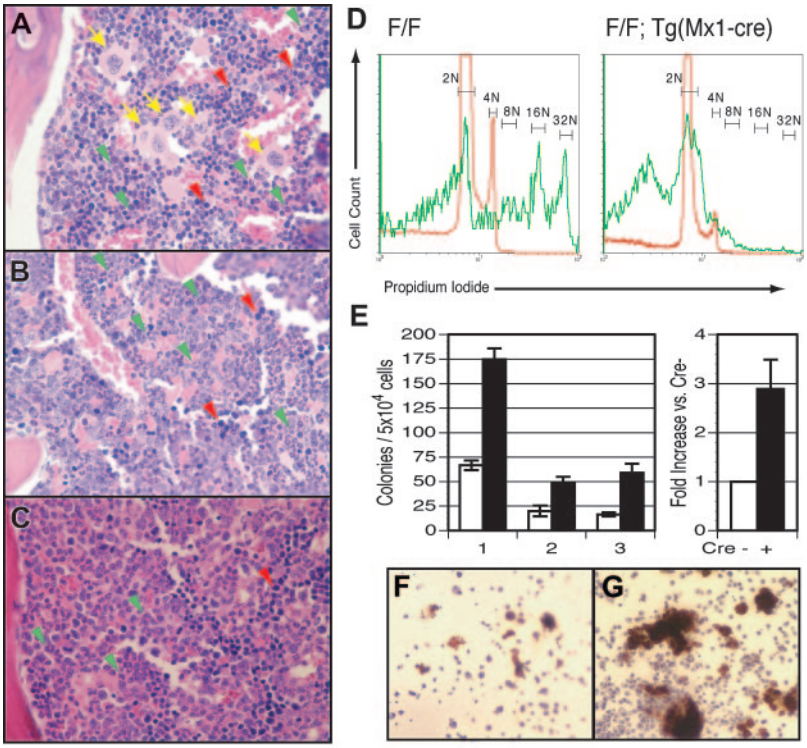

Figure 4. Megakaryocyte maturation is inefficient in plpC-treated *Runx1*-excised mice. BM from representative (A) *Runx1*$^{F/F}$ and (B) *Runx1*$^{F/F}$—Tg(*Mx1*-Cre) mice 143 days after plpC injection shows an absence of normal megakaryocytes in *Runx1*-excised mice (hematoxylin and eosin [H&E] staining; original magnification, × 600). (C) BM from representative *Runx1*$^{F/F}$—Tg(*Mx1*-Cre) recipient mice 98 days after transplantation (H&E; original magnification, × 600). (A-C) Yellow arrows indicate representative megakaryocytes. Red and green arrowheads indicate representative erythroid and myeloid elements, respectively. Sections demonstrate a notable absence of megakaryocytes and an increased ratio of maturing myeloid-to-erythroid forms in *Runx1*-excised versus nonexcised marrows. (D) Histograms depicting number of cultured *Runx1*$^{F/F}$ and *Runx1*$^{F/F}$—Tg (*Mx1*-Cre) bone marrow cells stained with propidium iodide to show ploidy. Colors indicate CD41 gates: green, CD41$^+$; red, CD41$^-$. (E, left) Plotted are mean ± SD numbers of acetylcholinesterase-positive colonies per 5×10^4 BM cells plated from plpC-treated *Runx1*$^{F/F}$ (□) and *Runx1*$^{F/F}$—Tg(*Mx1*-Cre) (■) mice. Results shown are for 3 experiments performed in quadruplicate. 1 and 3, fresh marrow; 2, previously frozen marrow. (Right) Plotted is the average fold increase for *Runx1*$^{F/F}$—Tg(*Mx1*-Cre) (■) relative to *Runx1*$^{F/F}$ (□) in the 3 experiments ($P \leq .034$). Representative megakaryocyte colonies from (F) *Runx1*$^{F/F}$ and (G) *Runx1*$^{F/F}$—Tg(*Mx1*-Cre) mice show acetylcholinesterase staining (brown) of megakaryocytic cells (original magnification, × 100).

showed reduced polyploidization of CD41$^+$ BM cells (Figure 4D). However, we paradoxically observed that in vitro megakaryocyte colony-plating efficiency was increased by an average of 2.9 (± 0.6)–fold (Figure 4E). Furthermore, megakaryocytic colonies displayed an increased number of acetylcholinesterase-positive cells per colony (Figure 4F-G).

Immunophenotypic analysis of myeloid progenitors derived from BM showed that the CMP population (IL-7Rα$^-$Lin$^-$Sca-1$^-$c-Kit$^+$CD34$^+$FcγRII/III$^+$) was not significantly altered in *Runx1*-excised mice. However, the GMP population (IL-7Rα$^-$Lin$^-$Sca-1$^-$c-Kit$^+$CD34$^+$FcγRII/III^{hi}) was expanded approximately 3-fold ($P = .032$) in *Runx1*-excised mice (Table 1). These observations are consistent with the increased production of myeloid colonies in vitro (Figure 5A). Unfractionated BM derived from plpC-treated *Runx1*$^{F/F}$—Tg(*Mx1*-Cre) mice had an approximately 3.4-fold increase in total myeloid colonies relative to plpC-treated *Runx1*$^{F/F}$ mice. Microscopic evaluation of Wright-Giemsa–stained cytospins of granulocyte-macrophage (GM) and mixed-lineage colonies indicated that *Runx1*-excised colonies gave rise to the full range of myeloid cell types observed in control colonies (Figure 5B). GM and mixed-lineage colonies were increased 3.9- and 3.2-fold compared with controls, respectively. In contrast, there was no significant change in erythroid blast-forming unit (BFU-E) colony number. Evaluation of individual colonies by PCR indicated complete *Runx1* excision in 92% of evaluable colonies from plpC-treated *Runx1*$^{F/F}$—Tg(*Mx1*-Cre) mice (Figure 5C) compared with *Runx1*$^{F/F}$ controls.

Perhaps the most unexpected finding in adult *Runx1*-excised mice was a mild myeloid expansion in hematopoietic tissues. Histopathologic examination of *Runx1*-excised BM showed subtle myeloid hyperplasia with a consistent increase in the ratio of maturing myeloid to erythroid forms compared with controls (Figure 4A-B). *Runx1*-excised marrows were hypercellular, yielding twice as many cells as control marrows. Similar findings were observed in mice after noncompetitive transplantation (Figure 4C).

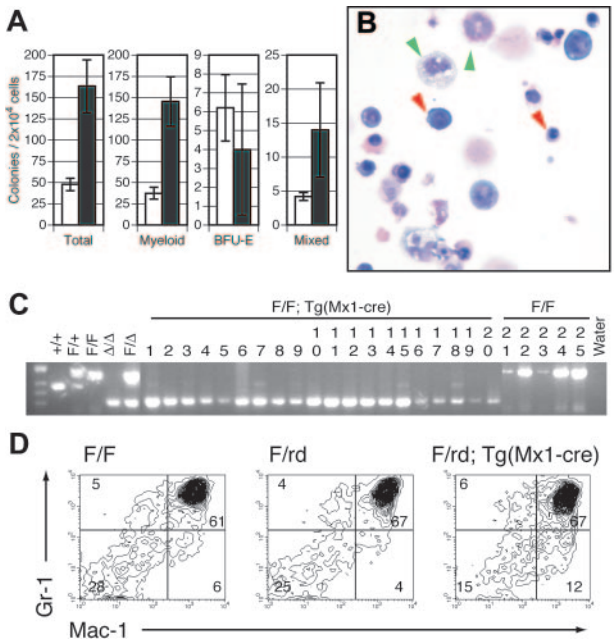

Figure 5. Mature and progenitor myeloid cell populations are expanded in plpC-treated *Runx1*-excised mice. (A) Plotted are the mean ± SD of total ($P < .05$), myeloid ($P < .05$), BFU-E ($P = .5$), and mixed-lineage colonies ($P = <.05$) per 2×10^4 BM cells plated in vitro from plpC-treated *Runx1*$^{F/F}$ (□) and *Runx1*$^{F/F}$—Tg(*Mx1*-Cre) (■) mice. Results are the average of 3 experiments performed in duplicate. (B) Representative cytospin from mixed-lineage colony derived from *Runx1*$^{F/F}$—Tg(*Mx1*-Cre) BM (Wright-Giemsa staining; original magnification, × 600). Red arrowheads indicate representative erythroid elements. Green arrowheads denote myeloid and monocytic forms. (C) Representative EtBr-stained 3% agarose gel of *Runx1* PCR products from single GM or mixed-lineage colonies derived from *Runx1*$^{F/F}$—Tg(*Mx1*-Cre) (lanes 1-20) and *Runx1*$^{F/F}$ (lanes 21-25) mice. Of 70 *Runx1*$^{F/F}$—Tg(*Mx1*-Cre) colonies evaluated, 9 (12.8%) failed to show any amplification, 5 of 61 (8.2%) indicated partial excision, and 56 of 61 (91.8%) were completely excised. Tail and embryo genomic DNA controls are as indicated. (D) Gr1 and Mac1 staining of BM from representative CXB6F1 mice 154 days after plpC induction. Numbers indicate percentages of cells gated in each respective quadrant.

Table 3. Spleen weights of plpC-treated mice

Genotype	No. mice	Days after plpC	Spleen weight, mg, mean ± SD	Fold increase
Runx1$^{F/F}$	7	60-273	153 ± 48	—
Runx1$^{F/F}$—Tg(*Mx1*-Cre)	9	91-273	318‡ ± 195	2.08
Runx1$^{F/+}$	4	154	122 ± 26	—
Runx1$^{F/rd}$ and *Runx1*$^{F/+}$—Tg(*Mx1*-Cre)	5	154	129 ± 14	—
Runx1$^{F/rd}$—Tg(*Mx1*-Cre)	6	154	185§ ± 42	1.52‖/1.43¶
Runx1$^{F/F}$ recipients*	2	98†	84 ± 21	—
Runx1$^{F/F}$—Tg(*Mx1*-Cre) recipients*	4	98†	128 ± 10	1.53

*Mice that underwent transplantation with *Runx1*$^{F/F}$ or *Runx1*$^{F/F}$Tg(*Mx1*-Cre) marrow in the absence of competitor marrow.
†Days after transplantation.
‡Comparison with *Runx1*$^{F/F}$ ($P < .01$; Mann-Whitney *U* test).
§Comparison with *Runx1*$^{F/+}$ ($P = .033$). Comparison with *Runx1*$^{F/rd}$ and *Runx1*$^{F/+}$—Tg(*Mx1*-Cre) ($P = .068$; Mann- Whitney *U* test).
‖Comparison with *Runx1*$^{F/+}$.
¶Comparison with *Runx1*$^{F/rd}$ and *Runx1*$^{F/+}$—Tg(*Mx1*-Cre).

The histopathologic findings were supported by a 2.4-fold expansion of Mac1$^+$ cells in excised BM of *Runx1*$^{F/F}$—Tg(*Mx1*-Cre) ($P = .021$) (data not shown) and *Runx1*$^{F/rd}$—Tg(*Mx1*-Cre) ($P = .021$) (Figure 5D) compared with controls.

Gross and histopathologic findings consistent with a myeloproliferative phenotype included splenomegaly attributable to extramedullary hematopoiesis in the spleen, with an increase in spleen weight of 1.4- to 2.1-fold in *Runx1*-excised mice compared with controls (Table 3). Histopathologic examination of spleen sections showed effacement of splenic architecture with a mild expansion of the red pulp resulting from extramedullary hematopoiesis composed predominantly of maturing myeloid forms and admixed erythroid elements, with only scant to rare megakaryocytes (Figure 6A-B). Liver sections from *Runx1*-excised mice also showed extramedullary hematopoiesis composed of maturing myeloid elements in a perivascular distribution (Figure 6C-D). Spleens of mice that underwent transplantation with excised *Runx1*$^{F/F}$—Tg(*Mx1*-Cre) marrow in the absence of wild-type competitor cells also demonstrated extramedullary hematopoiesis (Figure 6E-F). Flow cytometric analysis of single cell suspensions derived from spleens of primary *Runx1*-excised animals and animals that underwent transplantation with *Runx1*-excised BM confirmed the increase of myeloid lineage cells in the spleen (Figure 6G; Table 4). In *Runx1*$^{F/F}$—Tg(*Mx1*-Cre) mice and mice after transplantation, but not in *Runx1*$^{F/rd}$—Tg(*Mx1*-Cre) mice, there was a significant expansion of CD45$^-$Ter119$^+$ cells in the spleen (Figure 6G; Table 4). Taken together, these data indicate that *Runx1* is not required for neutrophil development, but its loss of function contributes to a myeloproliferative phenotype.

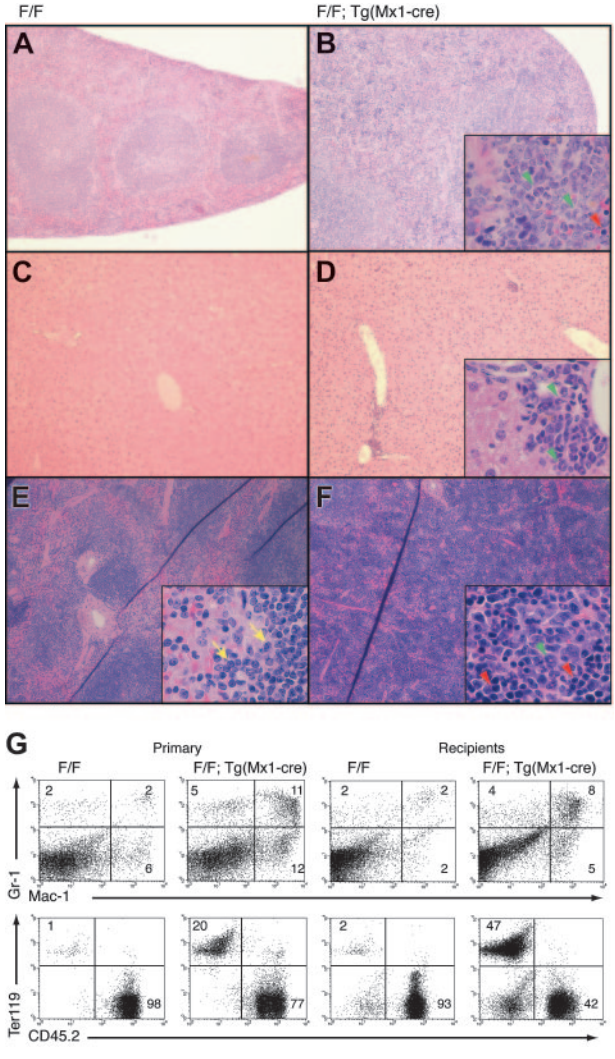

Figure 6. *Runx1*-excised mice display myeloid expansion in spleen and liver. Spleen (A-B) and liver (C-D) sections from representative (A,C) *Runx1*$^{F/F}$ and (B,D) *Runx1*$^{F/F}$—Tg(*Mx1*-Cre) mice 143 days after plpC (H&E; original magnification, ×100). Insets' original magnification, × 600. (E-F) Spleen sections from representative mice 14 weeks after transplantation with (E) *Runx1*$^{F/F}$ and (F) *Runx1*$^{F/F}$—Tg(*Mx1*-Cre) marrow (H&E; original magnification, × 100). Insets' original magnification, ×600. (A-F) Yellow arrows indicate representative lymphocytes. Red and green arrowheads indicate representative erythroid and myeloid elements, respectively. Sections demonstrate the presence of extramedullary hematopoiesis in the liver and splenic red pulp in *Runx1*-excised mice, absent in nonexcised control animals. (G) Gr1/Mac1 and CD45.2/Ter119 staining of splenocytes of indicated genotype from representative primary mice or mice that underwent transplantation. Numbers indicate percentage of cells gated in each respective quadrant.

Discussion

Runx1 deficiency during development results in a failure of HSC emergence and lethal central nervous system (CNS) hemorrhage, but the data presented here indicate that *Runx1* is not required in the adult murine hematopoietic compartment for HSC maintenance or survival of adult mice. However, there were a number of mild to severe hematopoietic abnormalities, including a block in lymphoid development, reduced platelet production, and development of a myeloproliferative phenotype.

Runx1-excised adult mice have an expanded, immunophenotypically defined HSC compartment. These mice survive with a follow-up of more than 5 months, indicating that there is long-term HSC activity in these animals. This finding is surprising in light of the hematopoietic defect observed in *Runx1*-deficient embryos. We

Table 4. Myeloid expansion in spleens of *Runx1*-excised mice

Genotype	No. mice	Time after pIpC, d	Gr1$^+$ splenocytes, mean ± SD, %* (*P*)	Gr1$^+$Mac1$^+$ splenocytes, mean ± SD, %* (*P*)	Mac1$^+$ splenocytes, mean ± SD, %* (*P*)	Ter119$^+$/CD45$^-$ splenocytes, mean ± SD, %* (*P*)†
Runx1$^{F/F}$‡	4	186-190	2.9 ± 0.6 (.999‖¶)	1.6 ± 0.4 (.008‖)	6.1 ± 1.4 (.014‖)	2.9 ± 1.6 (.023‖)
Runx1$^{F/F}$—Tg(*Mx1*-Cre)‡	7	186-190	2.7 ± 1.9	10.2 ± 4.7	14.9 ± 8.8	20.6 ± 15.5
Runx1$^{F/+}$	4	154	5.7 ± 1.5 (.020#)	2.5 ± 0.2 (.020#)	1.8 ± 0.2 (.020#)	2.0 ± 1.3 (.136¶#)
Runx1$^{F/+}$—Tg(*Mx1*-Cre) and *Runx1*$^{F/rd}$	5	154	7.5 ± 1.2 (.465¶**)	5.4 ± 2.8 (.029**)	12.0 ± 0.6 (.006**)	3.1 ± 2.1 (.715¶**)
Runx1$^{F/rd}$—Tg(*Mx1*-Cre)	6	154	8.3 ± 1.2	12.7 ± 5.3	4.0 ± 0.5	3.8 ± 2.0
Runx1$^{F/F}$ (recipient)‡	2	96§	3.1 ± 1.2 (.098¶††)	2.5 ± 0.1 (.040††)	1.9 ± 0.5 (.061¶††)	2.8 ± 1.7 (.003††)
Runx1$^{F/F}$—Tg(*Mx1*-Cre) (recipient)‡	4	96§	5.8 ± 1.6	7.4 ± 2.2	3.9 ± 1.0	50.0 ± 9.3

*Numbers indicate mean percentage Mac1$^+$, Gr1$^+$, or Mac1$^+$Gr1$^+$ of total splenocytes. Primary pIpC-treated splenocytes were stained with CD45.2- FITC, Mac1-PE, 7AAD-PerCP-Cy5.5, and Gr1-APC and were gated by scatter and 7AAD negativity. Splenocytes from animals that underwent transplantation were stained with CD45.2-FITC, Mac1-PE, CD45.2-PerCP-Cy5.5, and Gr1-APC and were scatter gated.

†Numbers indicate mean percentage CD45$^-$Ter119$^+$ of total splenocytes. Splenocytes were stained with CD45.2-FITC, c-Kit-PE, 7AAD-PerCP- Cy5.5, and Ter119-APC. Splenocytes were gated by scatter and 7AAD negativity.

‡Representative data in Figure 6.

§Days after transplantation.

‖Mann-Whitney *U* test for comparison of primary *Runx1*$^{F/F}$—Tg(*Mx1*-Cre) to primary *Runx1*$^{F/F}$ animals.

¶Not statistically significant.

#Mann-Whitney *U* test for comparison of primary *Runx1*$^{F/rd}$—Tg(*Mx1*-Cre) to primary *Runx1*$^{F/+}$ animals.

**Mann-Whitney *U* test for comparison of primary *Runx1*$^{F/rd}$—Tg(*Mx1*-Cre) to primary *Runx1*$^{F/+}$—Tg(*Mx1*-Cre) and *Runx1*$^{F/rd}$ animals.

††Unpaired *t* test for comparison of mice that underwent transplantation with *Runx1*$^{F/F}$—Tg(*Mx1*-Cre) to mice that underwent transplantation with *Runx1*$^{F/F}$ animals.

note that homozygous loss of RUNX1 has been observed in humans with AML, though not in those with acute lymphoid leukemia.[38] These observations suggest that AML cells with self-renewal ability and limited ability to differentiate also do not require RUNX1. Our findings that *Runx1* is not required for HSC maintenance and survival in the adult are consistent with the persistence of RUNX1-deficient cells in human leukemias. BM transplantation studies indicate that *Runx1*-excised HSCs are competent for long-term repopulation. However, competitive repopulation studies indicate a significant reduction in *Runx1*-deficient HSC ability to compete with wild-type HSCs during repopulation.

Runx1 is required for efficient lymphoid maturation at multiple stages of differentiation. We observed a significant reduction in the number mature PB B cells and BM-derived B-cell precursors in primary *Runx1*-excised mice. This suggests a significant block in B-cell maturation, though it is unclear at which stage of B-cell maturation *Runx1* functions. In the T-cell lineage, we report a specific block in T-cell maturation during the transition from the DN2 (CD44$^+$CD25$^+$) to the DN3 (CD44$^-$CD25$^+$) stage.[56] This is consistent with reports describing a tightly regulated expression pattern for *Runx1* and CBFβ in developing thymocytes.[6,7,15,16,58] However, in contrast to the findings of Ichikawa et al,[56] we observed a significant reduction in bone marrow CLP, suggesting that *Runx1* is also important during the earliest stages of lymphoid lineage development. The difference in CLP production we observed compared with the observations of Ichikawa et al[56] may be the result of higher pIpC dosing in our study, resulting in more efficient excision, although other explanations are possible. Noncompetitive reconstitution assays indicate that *Runx1* is not required for commitment to and maturation of the lymphoid lineage. It is clear that the loss of *Runx1* severely reduces the efficiency of CLP production and lymphocyte maturation. This conclusion is supported by the clinical observation that RUNX1 loss is not observed in patients with acute lymphoblastic leukemia (ALL).

In contrast to the pronounced inhibition of the lymphoid lineage, excision of *Runx1* did not inhibit maturation of the myeloid lineage. *Runx1* loss had no apparent effect on the erythroid lineage, but it did have a significant effect on megakaryocytic maturation. *Runx1* is required for normal maturation of the megakaryocyte lineage but not for the establishment of this lineage. These differential requirements for *Runx1* in erythroid and megakaryocyte maturation correlate with reports that the expression of Runx1 and its heterodimeric binding partner, CBFβ, are markedly decreased in erythroid lineages[15,16,59] but are maintained in megakaryocytes.[16,59,60] Humans with FPD/AML syndrome have heterozygous loss of *RUNX1*, with an associated quantitative and qualitative platelet defect, and a proclivity to develop AML.[35] The platelet defect is reminiscent of the abnormalities observed in mice with homozygous loss of *Runx1* and suggests that there may be compensation in mice for monoallelic loss of *Runx1*.

RUNX1 loss in humans is most often associated with M0 (undifferentiated) AML, suggesting that RUNX1 loss may have deleterious effects on hematopoietic differentiation.[61,62] In contrast, *Runx1*-excised mice demonstrate expansion of the myeloid lineage by several phenotypic and functional criteria, with no evidence of a block in myeloid development. The specific expansion of the GMP, but not the CMP, population suggests that the myeloid expansion observed in *Runx1*-excised animals results from the loss of negative regulatory functions of *Runx1* in the GMP population. The strain-specific differences in expansion of CD45$^-$—Ter119$^+$ cells in the spleens of *Runx1*-excised mice indicate that the myeloid expansion is not secondary to a compensatory drive for increased platelet production. Although these findings are surprising, there have been several other indications that *Runx1* is not essential for adult hematopoiesis in mice. For example, expression of the leukemogenic fusion protein RUNX1-ETO, a dominant-negative inhibitor of CBF, during development results in an embryonic lethal phenotype with a lack of definitive hematopoiesis that is nearly identical to that observed in *Runx1*-deficient mice.[44,45] However, expression of Runx1-*ETO* from a conditional allele in the adult hematopoietic compartment has only subtle effects on hematopoiesis, characterized by enhanced replating efficiency of myeloid progenitors in vitro and an increased susceptibility to develop leukemia after *N*-ethyl-*N*-nitrosurea (ENU) mutagenesis.[63] *Runx1-ETO* or *Runx1*-deficient animals do not develop leukemia, suggesting that *Runx1* loss of function must be complemented with additional leukemogenic genetic events for the development of a leukemia phenotype. The myeloproliferative phenotype associated with *Runx1* excision suggests that *Runx1* loss may constitute a preleukemic state, and it may explain the

proclivity for the development of myeloid leukemias in the context of RUNX1 deficiency in humans. The ability of *Runx1*-deficient myeloid lineage cells to differentiate normally suggests that the block in differentiation observed in leukemias with loss of RUNX1 function cannot be attributed to the loss of RUNX1 alone and that it must be due to other genetic events.

Acknowledgments

We thank Woo Jong Song, Terryl Stacy, Vivienne Rebel, and Hanno Hock for their insightful discussions and contributions to the completion of this work.

References

1. North T, Gu TL, Stacy T, et al. Cbfa2 is required for the formation of intra-aortic hematopoietic clusters. Development. 1999;126:2563-2575.
2. Cai Z, de Bruijn M, Ma X, et al. Haploinsufficiency of AML1 affects the temporal and spatial generation of hematopoietic stem cells in the mouse embryo. Immunity. 2000;13:423-431.
3. Cameron S, Taylor DS, TePas EC, Speck NA, Mathey-Prevot B. Identification of a critical regulatory site in the human interleukin-3 promoter by in vivo footprinting. Blood. 1994;83:2851-2859.
4. Otto F, Lubbert M, Stock M. Upstream and downstream targets of RUNX proteins. J Cell Biochem. 2003;89:9-18.
5. de Bruijn MF, Speck NA. Core-binding factors in hematopoiesis and immune function. Oncogene. 2004;23:4238-4248.
6. Taniuchi I, Osato M, Egawa T, et al. Differential requirements for Runx proteins in CD4 repression and epigenetic silencing during T lymphocyte development. Cell. 2002;111:621-633.
7. Woolf E, Xiao C, Fainaru O, et al. Runx3 and Runx1 are required for CD8 T cell development during thymopoiesis. Proc Natl Acad Sci U S A. 2003;100:7731-7736.
8. Lauzurica P, Zhong XP, Krangel MS, Roberts JL. Regulation of T cell receptor delta gene rearrangement by CBF/PEBP2. J Exp Med. 1997; 185:1193-1201.
9. Takahashi A, Satake M, Yamaguchi-Iwai Y, et al. Positive and negative regulation of granulocyte-macrophage colony-stimulating factor promoter activity by AML1-related transcription factor, PEBP2. Blood. 1995;86:607-616.
10. Zhang DE, Fujioka K, Hetherington CJ, et al. Identification of a region which directs the monocytic activity of the colony-stimulating factor 1 (macrophage colony-stimulating factor) receptor promoter and binds PEBP2/CBF (AML1). Mol Cell Biol. 1994;14:8085-8095.
11. Wang Q, Stacy T, Binder M, Marin-Padilla M, Sharpe AH, Speck NA. Disruption of the *Cbfa2* gene causes necrosis and hemorrhaging in the central nervous system and blocks definitive hematopoiesis. Proc Natl Acad Sci U S A. 1996;93: 3444-3449.
12. Wang Q, Stacy T, Miller JD, et al. The CBFbeta subunit is essential for CBFalpha2 (AML1) function in vivo. Cell. 1996;87:697-708.
13. Okuda T, van Deursen J, Hiebert SW, Grosveld G, Downing JR. AML1, the target of multiple chromosomal translocations in human leukemia, is essential for normal fetal liver hematopoiesis. Cell. 1996;84:321-330.
14. Sasaki K, Yagi H, Bronson RT, et al. Absence of fetal liver hematopoiesis in mice deficient in transcriptional coactivator core binding factor beta. Proc Natl Acad Sci U S A. 1996;93:12359-12363.
15. Lorsbach RB, Moore J, Ang SO, Sun W, Lenny N, Downing JR. Role of RUNX1 in adult hematopoiesis: analysis of RUNX1-IRES-GFP knock-in mice reveals differential lineage expression. Blood. 2004;103:2522-2529.
16. North TE, Stacy T, Matheny CJ, Speck NA, de Bruijn MF. Runx1 is expressed in adult mouse hematopoietic stem cells and differentiating myeloid and lymphoid cells, but not in maturing erythroid cells. Stem Cells. 2004;22:158-168.
17. Miyoshi H, Shimizu K, Kozu T, Maseki N, Kaneko Y, Ohki M. t(8;21) breakpoints on chromosome 21 in acute myeloid leukemia are clustered within a limited region of a single gene, AML1. Proc Natl Acad Sci U S A. 1991;88:10431-10434.
18. Miyoshi H, Kozu T, Shimizu K, et al. The t(8;21) translocation in acute myeloid leukemia results in production of an AML1-MTG8 fusion transcript. EMBO J. 1993;12:2715-2721.
19. Nucifora G, Birn DJ, Erickson P, et al. Detection of DNA rearrangements in the AML1 and ETO loci and of an AML1/ETO fusion mRNA in patients with t(8;21) acute myeloid leukemia. Blood. 1993; 81:883-888.
20. Erickson P, Gao J, Chang KS, et al. Identification of breakpoints in t(8;21) acute myelogenous leukemia and isolation of a fusion transcript, AML1/ETO, with similarity to *Drosophila* segmentation gene, *runt*. Blood. 1992;80:1825-1831.
21. Nisson PE, Watkins PC, Sacchi N. Transcriptionally active chimeric gene derived from the fusion of the *AML1* gene and a novel gene on chromosome 8 in t(8;21) leukemic cells. Cancer Genet Cytogenet. 1992;63:81-88.
22. Liu P, Tarle SA, Hajra A, et al. Fusion between transcription factor CBF beta/PEBP2 beta and a myosin heavy chain in acute myeloid leukemia. Science. 1993;261:1041-1044.
23. Golub TR, Barker GF, Bohlander SK, et al. Fusion of the *TEL* gene on 12p13 to the *AML1* gene on 21q22 in acute lymphoblastic leukemia. Proc Natl Acad Sci U S A. 1995;92:4917-4921.
24. Romana SP, Mauchauffe M, Le Coniat M, et al. The t(12;21) of acute lymphoblastic leukemia results in a *tel-AML1* gene fusion. Blood. 1995;85: 3662-3670.
25. Shurtleff SA, Buijs A, Behm FG, et al. TEL/AML1 fusion resulting from a cryptic t(12;21) is the most common genetic lesion in pediatric ALL and defines a subgroup of patients with an excellent prognosis. Leukemia. 1995;9:1985-1989.
26. Tien HF, Wang CH, Lin MT, et al. Correlation of cytogenetic results with immunophenotype, genotype, clinical features, and ras mutation in acute myeloid leukemia: a study of 235 Chinese patients in Taiwan. Cancer Genet Cytogenet. 1995; 84:60-68.
27. Langabeer SE, Walker H, Gale RE, et al. Frequency of CBF beta/MYH11 fusion transcripts in patients entered into the U.K. MRC AML trials: the MRC Adult Leukaemia Working Party. Br J Haematol. 1997;96:736-739.
28. Grimwade D, Walker H, Oliver F, et al. The importance of diagnostic cytogenetics on outcome in AML: analysis of 1,612 patients entered into the MRC AML 10 trial: the Medical Research Council Adult and Children's Leukaemia Working Parties. Blood. 1998;92:2322-2333.
29. Langabeer SE, Walker H, Rogers JR, et al. Incidence of AML1/ETO fusion transcripts in patients entered into the MRC AML trials: MRC Adult Leukaemia Working Party. Br J Haematol. 1997;99: 925-928.
30. Rowe D, Cotterill SJ, Ross FM, et al. Cytogenetically cryptic AML1-ETO and CBF beta-MYH11 gene rearrangements: incidence in 412 cases of acute myeloid leukaemia. Br J Haematol. 2000; 111:1051-1056.
31. Loh ML, Silverman LB, Young ML, et al. Incidence of TEL/AML1 fusion in children with relapsed acute lymphoblastic leukemia. Blood. 1998;92:4792-4797.
32. Liang DC, Chou TB, Chen JS, et al. High incidence of TEL/AML1 fusion resulting from a cryptic t(12;21) in childhood B-lineage acute lymphoblastic leukemia in Taiwan. Leukemia. 1996;10: 991-993.
33. Harbott J, Viehmann S, Borkhardt A, Henze G, Lampert F. Incidence of TEL/AML1 fusion gene analyzed consecutively in children with acute lymphoblastic leukemia in relapse. Blood. 1997; 90:4933-4937.
34. Borkhardt A, Cazzaniga G, Viehmann S, et al. Incidence and clinical relevance of TEL/AML1 fusion genes in children with acute lymphoblastic leukemia enrolled in the German and Italian multicenter therapy trials: Associazione Italiana Ematologia Oncologia Pediatrica and the Berlin-Frankfurt-Munster Study Group. Blood. 1997;90: 571-577.
35. Song WJ, Sullivan MG, Legare RD, et al. Haploinsufficiency of CBFA2 causes familial thrombocytopenia with propensity to develop acute myelogenous leukaemia. Nat Genet. 1999;23:166-175.
36. Michaud J, Wu F, Osato M, et al. In vitro analyses of known and novel RUNX1/AML1 mutations in dominant familial platelet disorder with predisposition to acute myelogenous leukemia: implications for mechanisms of pathogenesis. Blood. 2002;99:1364-1372.
37. Preudhomme C, Warot-Loze D, Roumier C, et al. High incidence of biallelic point mutations in the Runt domain of the AML1/PEBP2 alpha B gene in Mo acute myeloid leukemia and in myeloid malignancies with acquired trisomy 21. Blood. 2000; 96:2862-2869.
38. Osato M, Asou N, Abdalla E, et al. Biallelic and heterozygous point mutations in the runt domain of the AML1/PEBP2alphaB gene associated with myeloblastic leukemias. Blood. 1999;93:1817-1824.
39. Fenrick R, Amann JM, Lutterbach B, et al. Both TEL and AML-1 contribute repression domains to the t(12;21) fusion protein. Mol Cell Biol. 1999;19: 6566-6574.
40. Hiebert SW, Sun W, Davis JN, et al. The t(12;21) translocation converts AML-1B from an activator to a repressor of transcription. Mol Cell Biol. 1996;16:1349-1355.
41. Lutterbach B, Westendorf JJ, Linggi B, et al. ETO, a target of t(8;21) in acute leukemia, interacts with the N-CoR and mSin3 corepressors. Mol Cell Biol. 1998;18:7176-7184.
42. Westendorf JJ, Yamamoto CM, Lenny N, Downing JR, Selsted ME, Hiebert SW. The t(8;21) fusion product, AML-1-ETO, associates with C/EBP-alpha, inhibits C/EBP-alpha-dependent transcription, and blocks granulocytic differentiation. Mol Cell Biol. 1998;18:322-333.
43. Castilla LH, Wijmenga C, Wang Q, et al. Failure of embryonic hematopoiesis and lethal hemorrhages in mouse embryos heterozygous for a knocked-in leukemia gene CBFB-MYH11. Cell. 1996;87:687-696.
44. Yergeau DA, Hetherington CJ, Wang Q, et al. Embryonic lethality and impairment of haematopoiesis in mice heterozygous for an AML1-ETO fusion gene. Nat Genet. 1997;15:303-306.
45. Okuda T, Cai Z, Yang S, et al. Expression of a

knocked-in AML1-ETO leukemia gene inhibits the establishment of normal definitive hematopoiesis and directly generates dysplastic hematopoietic progenitors. Blood. 1998;91:3134-3143.

46. Mikkola HK, Klintman J, Yang H, et al. Haematopoietic stem cells retain long-term repopulating activity and multipotency in the absence of stem-cell leukaemia *SCL/tal-1* gene. Nature. 2003;421:547-551.
47. Hall MA, Curtis DJ, Metcalf D, et al. The critical regulator of embryonic hematopoiesis, SCL, is vital in the adult for megakaryopoiesis, erythropoiesis, and lineage choice in CFU-S12. Proc Natl Acad Sci U S A. 2003;100:992-997.
48. Curtis DJ, Hall MA, Van Stekelenburg LJ, Robb L, Jane SM, Begley CG. SCL is required for normal function of short-term repopulating hematopoietic stem cells. Blood. 2004;103:3342-3348.
49. Kuhn R, Schwenk F, Aguet M, Rajewsky K. Inducible gene targeting in mice. Science. 1995;269:1427-1429.
50. Liu Q, Schwaller J, Kutok J, et al. Signal transduction and transforming properties of the TEL-TRKC fusions associated with t(12;15)(p13;q25) in congenital fibrosarcoma and acute myelogenous leukemia. EMBO J. 2000;19:1827-1838.
51. Schwaller J, Frantsve J, Aster J, et al. Transformation of hematopoietic cell lines to growth-factor independence and induction of a fatal myelo- and lymphoproliferative disease in mice by retrovirally transduced TEL/JAK2 fusion genes. EMBO J. 1998;17:5321-5333.
52. Akashi K, Traver D, Miyamoto T, Weissman IL. A clonogenic common myeloid progenitor that gives rise to all myeloid lineages. Nature. 2000;404:193-197.
53. Kondo M, Weissman IL, Akashi K. Identification of clonogenic common lymphoid progenitors in mouse bone marrow. Cell. 1997;91:661-672.
54. Jackson CW, Brown LK, Somerville BC, Lyles SA, Look AT. Two-color flow cytometric measurement of DNA distributions of rat megakaryocytes in unfixed, unfractionated marrow cell suspensions. Blood. 1984;63:768-778.
55. Lakso M, Pichel JG, Gorman JR, et al. Efficient in vivo manipulation of mouse genomic sequences at the zygote stage. Proc Natl Acad Sci U S A. 1996;93:5860-5865
56. Ichikawa M, Asai T, Saito T, et al. AML-1 is required for megakaryocytic maturation and lymphocytic differentiation, but not for maintenance of hematopoietic stem cells in adult hematopoiesis. Nat Med. 2004;10:299-304.
57. Spangrude GJ, Scollay R. Differentiation of hematopoietic stem cells in irradiated mouse thymic lobes: kinetics and phenotype of progeny. J Immunol. 1990;145:3661-3668.
58. Kundu M, Liu PP. Cbf beta is involved in maturation of all lineages of hematopoietic cells during embryogenesis except erythroid. Blood Cells Mol Dis. 2003;30:164-169.
59. Kundu M, Chen A, Anderson S, et al. Role of Cbfb in hematopoiesis and perturbations of the leukemogenic fusion gene Cbfb-MYH11. Blood. 2002;100:2449-2456
60. Elagib KE, Racke FK, Mogass M, Khetawat R, Delehanty LL, Goldfarb AN. RUNX1 and GATA-1 coexpression and cooperation in megakaryocytic differentiation. Blood. 2003;101:4333-4341.
61. Roumier C, Eclache V, Imbert M, et al. M0 AML, clinical and biologic features of the disease, including *AML1* gene mutations: a report of 59 cases by the Groupe Francais d'Hematologie Cellulaire (GFHC) and the Groupe Francais de Cytogenetique Hematologique (GFCH). Blood. 2003;101:1277-1283.
62. Langabeer SE, Gale RE, Rollinson SJ, Morgan GJ, Linch DC. Mutations of the *AML1* gene in acute myeloid leukemia of FAB types M0 and M7. Genes Chromosomes Cancer. 2002;34:24-32.
63. Higuchi M, O'Brien D, Kumaravelu P, Lenny N, Yeoh EJ, Downing JR. Expression of a conditional AML1-ETO oncogene bypasses embryonic lethality and establishes a murine model of human t(8;21) acute myeloid leukemia. Cancer Cell. 2002;1:63-74.

2005 106: 494-504
doi:10.1182/blood-2004-08-3280 originally published online March 22, 2005

Loss of *Runx1* perturbs adult hematopoiesis and is associated with a myeloproliferative phenotype

Joseph D. Growney, Hirokazu Shigematsu, Zhe Li, Benjamin H. Lee, Jennifer Adelsperger, Rebecca Rowan, David P. Curley, Jeffery L. Kutok, Koichi Akashi, Ifor R. Williams, Nancy A. Speck and D. Gary Gilliland

Blood (print ISSN 0006-4971, online ISSN 1528-0020), is published weekly by the American Society of Hematology, 2021 L St, NW, Suite 900, Washington DC 20036.